

Electronic Supplementary Information (ESI) for

**Mechanistic insights and importance of hydrophobicity in cationic polymers for cancer therapy**

Nishant Kumar<sup>a</sup>, Kenji Oqmhula<sup>b</sup>, Kenta Hongo<sup>c</sup>, Kengo Takagi<sup>d</sup>, Shin-ichi Yusa<sup>d</sup>, Robin Rajan<sup>a\*</sup>, Kazuaki Matsumura<sup>a\*</sup>

<sup>a</sup>School of Materials Science, Japan Advanced Institute of Science and Technology, 1-1 Asahidai, Nomi, Ishikawa 923-1292, Japan

<sup>b</sup>School of Information Science, Japan Advanced Institute of Science and Technology, 1-1 Asahidai, Nomi, Ishikawa 923-1292, Japan

<sup>c</sup>Research Center for Advanced Computing Infrastructure, Japan Advanced Institute of Science and Technology, 1-1 Asahidai, Nomi, Ishikawa 923-1292, Japan

<sup>d</sup>Department of Applied Chemistry, Graduate School of Engineering, University of Hyogo, 2167 Shosha, Himeji, Hyogo 671-2280, Japan

## Method for modeling and the molecular dynamics

### Modeling of polymers

PAMPTMA and PAMPTMA-*r*-BuMA polymers were modeled using Polymer Builder tool in Materials Studio 2022.<sup>1</sup> The PAMPTMA homopolymer consists of 15 AMPTMA monomer units, whereas the PAMPTMA-*r*-BuMA random copolymer are constructed from 10 AMPTMA and 5 BuMA monomer units. To perform their MD simulations, force fields and point charges should be assigned to the resulting polymer structures.

To assign point charges to the polymer, we first divided the polymer into the constituent monomer fragments and then allocated point charges into the fragments. The point charges of the fragment were calculated by the restrained electrostatic potential (RESP) approach<sup>2</sup>: The monomers were first optimized with DFT calculations at the B3LYP<sup>3</sup>, 4/6-31G(d,p)<sup>4</sup>, <sup>5</sup> level of theory using Gaussian 2016<sup>6</sup>; their single point energy calculations for the electrostatic potentials were done using the same level of theory; the computed ESPs were converted to RESP charges using the antechamber program in Ambertools21; the resultant monomer RESP charges were assigned into the polymer.

A general AMBER force field (GAFF)<sup>7</sup> was applied to the PAMPTMA and PAMPTMA-*r*-BuMA polymers with the RESP charges by using the antechamber<sup>8</sup>, <sup>9</sup> and parmchk2<sup>9</sup> programs in Ambertools20.<sup>9</sup> Note that the Cl<sup>-</sup> ions were excluded from the polymers when applying GAFF to the polymers. The Cl anion ion was constrained to bind with the N cation ion in a harmonic potential with the equilibrium distance between the ions of 3.57 Å and the coupling constant of 10 kcal/mol Å<sup>-2</sup>. The equilibrium distance was obtained from the DFT simulation of the monomer fragment.

The PAMPTMA and PAMPTMA-*r*-BuMA polymers were placed in a 10 nm × 10 nm × 10 nm simulation cell. The polymers were solvated with aqueous KCl solution at 0.15 M, where 32,441 and 32,449 water molecules were included in the PAMPTMA and PAMPTMA-*r*-BuMA cases, respectively. A TIP3P force field and GAFF were applied to water molecules and K<sup>+</sup>/Cl<sup>-</sup> ions, respectively.

To obtain equilibrium structures of PAMPTMA and PAMPTMA-*r*-BuMA, we performed the NVT MD simulations with the Nose-Hoover thermostat at 310 K for 0.5 ns, followed by the NPT MD simulations with the Nose-Hoover thermostat at 310 K and the Parrinello-Rahman barostat at 1 bar for 50 ns. These equilibrated structures were used for constructing the polymer-membrane systems.

### **Modeling of membrane**

The membrane was treated as a lipid bilayer sheet composed of 1-palmitoyl-2-oleoyl-sn-glycero-3-phosphocholine (POPC). Using Membrane Builder<sup>10-13</sup> in CHARMM-GUI,<sup>7</sup> the bilayer was modeled and packed into a MD simulation cell of 9.4 nm × 9.4 nm × 14.0 nm. Here two monolayers are located at the center of the simulation cell in *z*-direction, where the monolayer consists of 128 POPC monomer units. The membrane was fully solvated with aqueous KCl solutions at 0.15 M, where 26,702 water molecules were included in the MD simulation cell. The Lipid17 force field was applied to the membrane. We performed the MD simulation in the NVT ensemble with the Berendsen thermostat at 310 K for 0.25 ns (2 fs time step), followed by the NPT ensemble with the Berendsen thermostat and barostat at 1 bar for 2.5 ns (2 fs time step). Furthermore, the equilibration of the membrane structure was performed using the MD simulations in the NPT ensemble with Nose-Hoover thermostat at 310 K and Parrinello-Rahman barostat at 1 bar for 2.5 ns (2 fs time step). Input files including NVT/NPT MD parameters were prepared by CHARMM-GUI Input Generator.<sup>14, 15</sup> The equilibrated membrane structure is used to perform the MD simulations of the polymer-membrane systems.

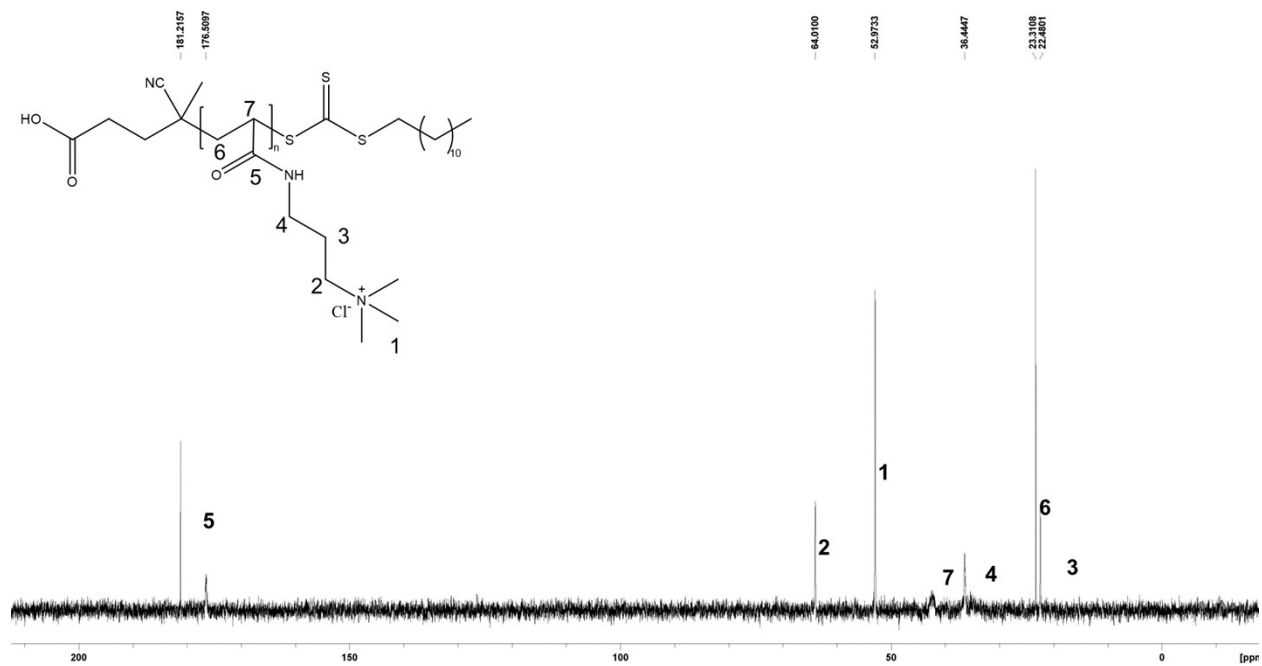
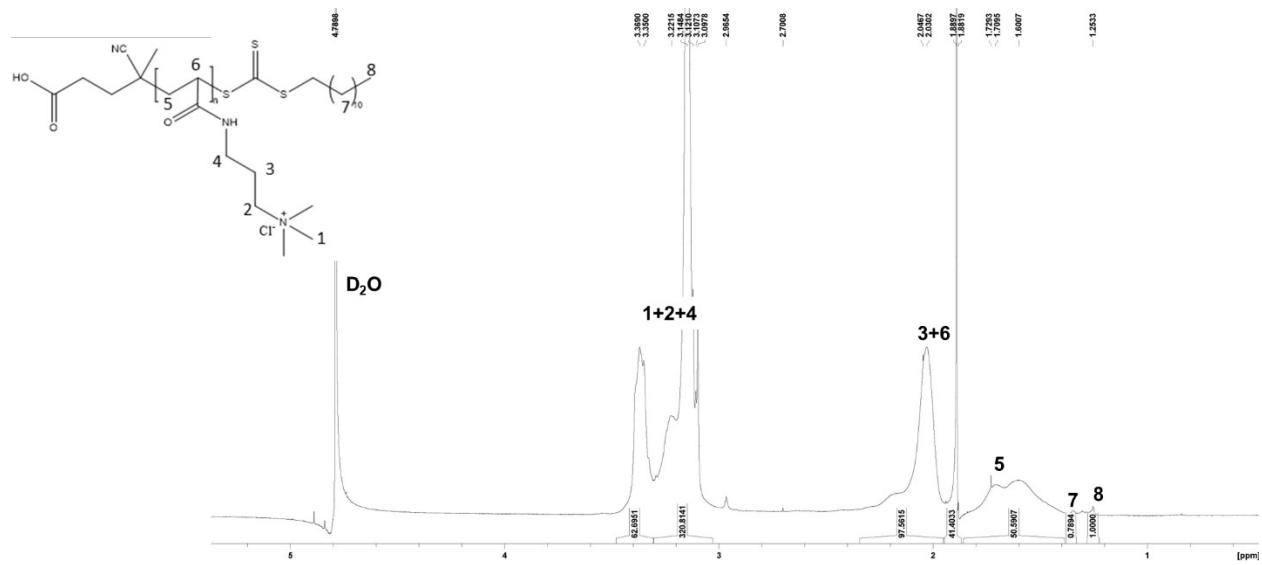


**Figure S1:** <sup>1</sup>H-NMR and <sup>13</sup>C-NMR of homopolymer of AMPTMA.

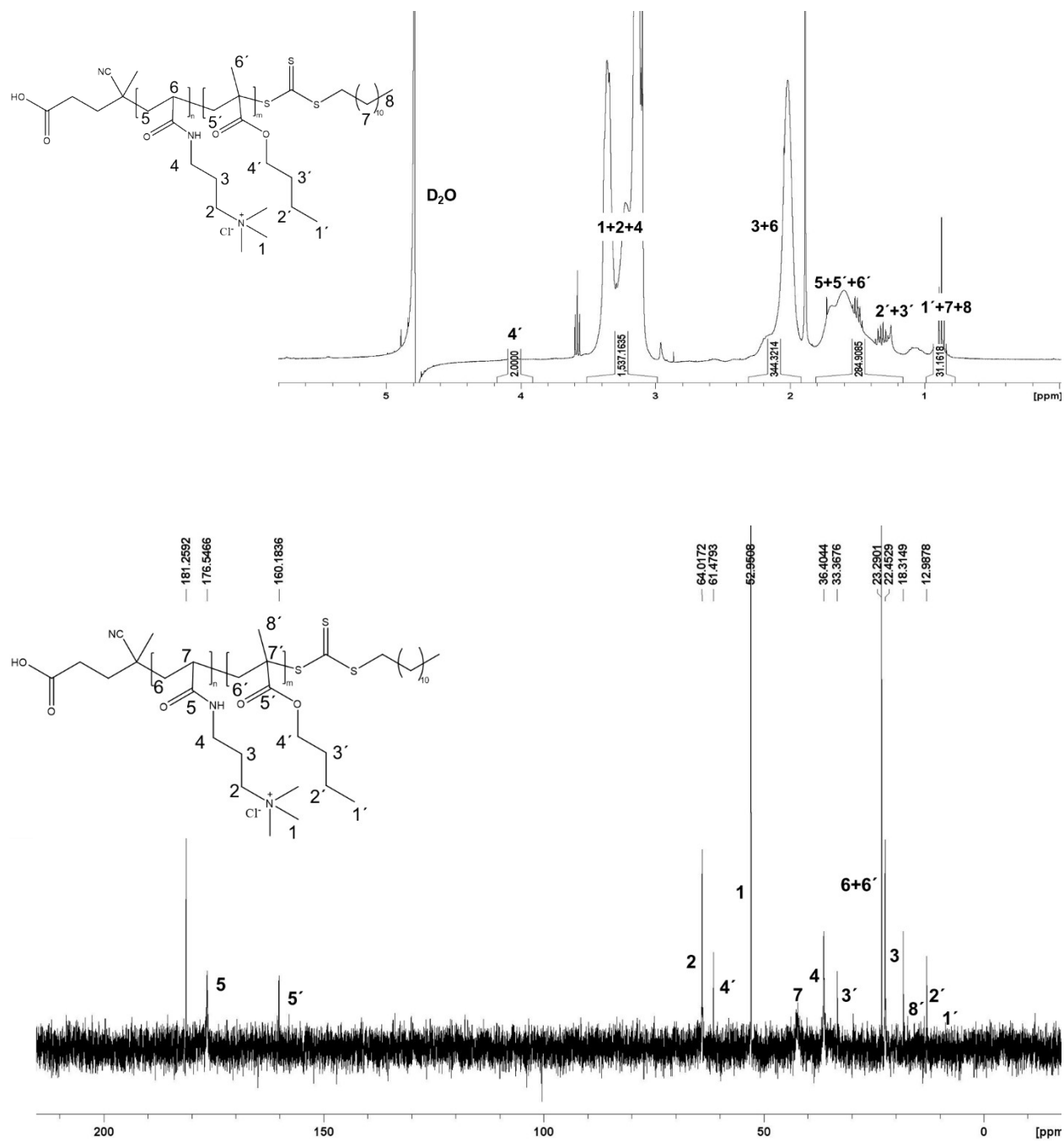


**Figure S2:** <sup>1</sup>H-NMR and <sup>13</sup>C-NMR of copolymer PAMPTMA-*r*-BuMA with 5 mol% of BuMA.

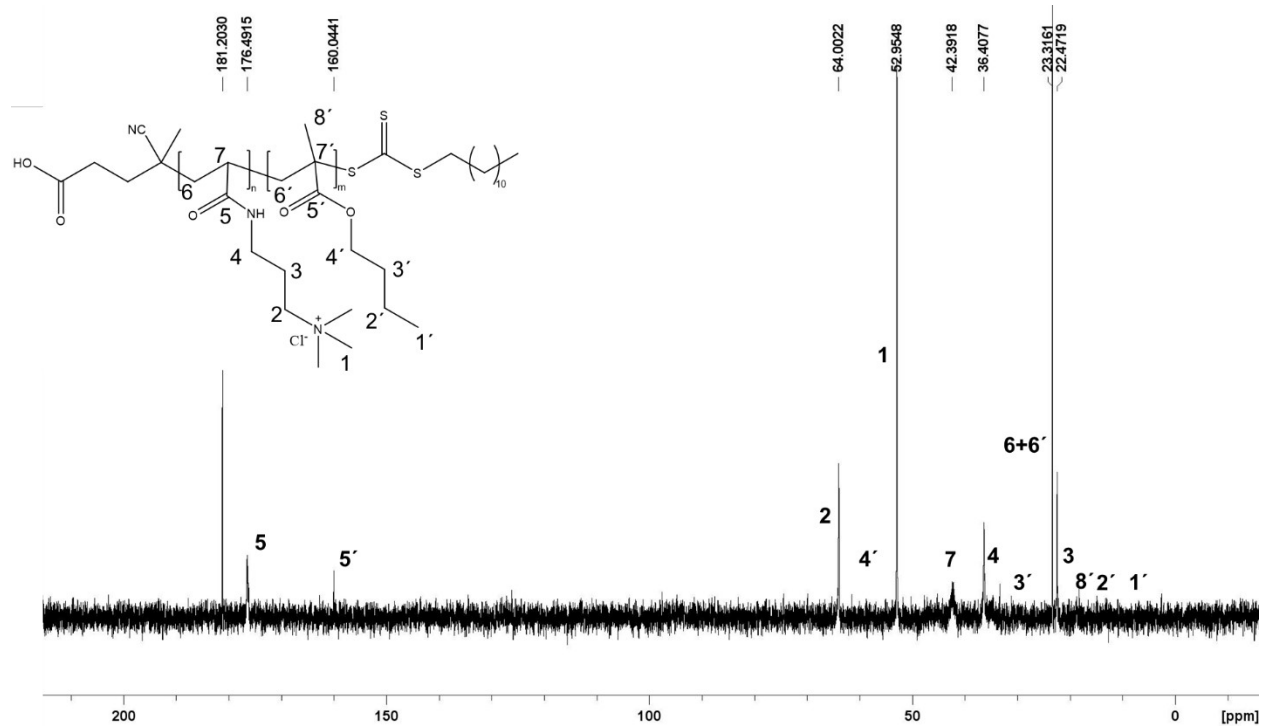
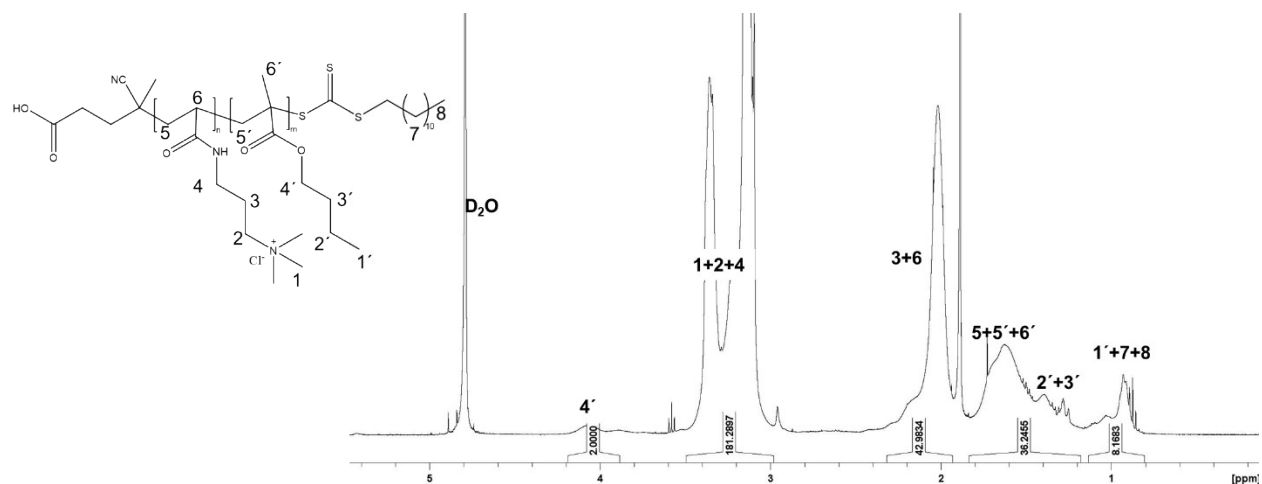


**Figure S3:** <sup>1</sup>H-NMR and <sup>13</sup>C-NMR of copolymer PAMPTMA-*r*-BuMA with 10 mol% of BuMA.

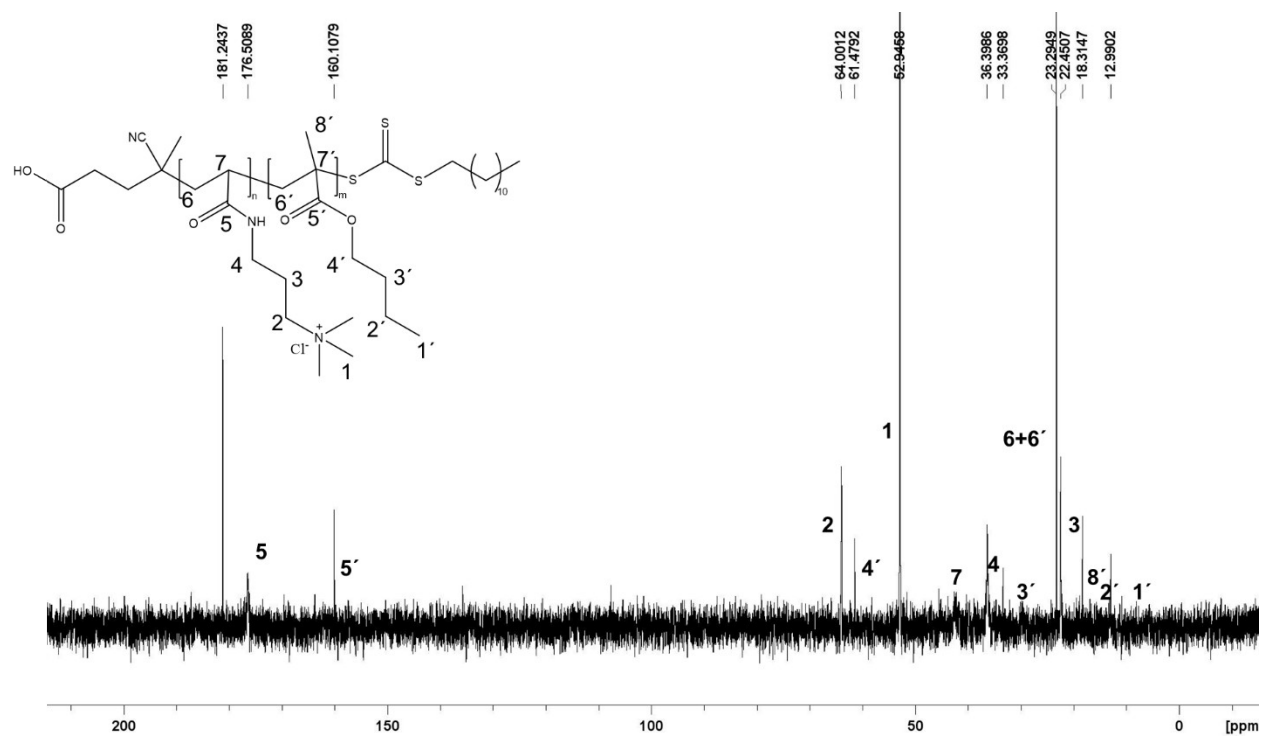
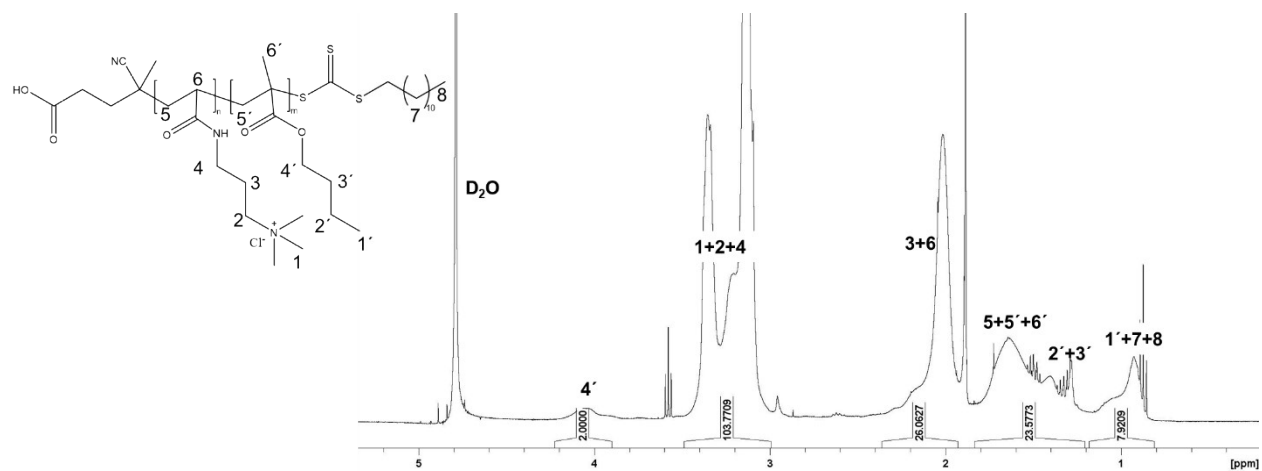


**Figure S4:** <sup>1</sup>H-NMR and <sup>13</sup>C-NMR of copolymer PAMPTMA-*r*-BuMA with 20 mol% of BuMA.

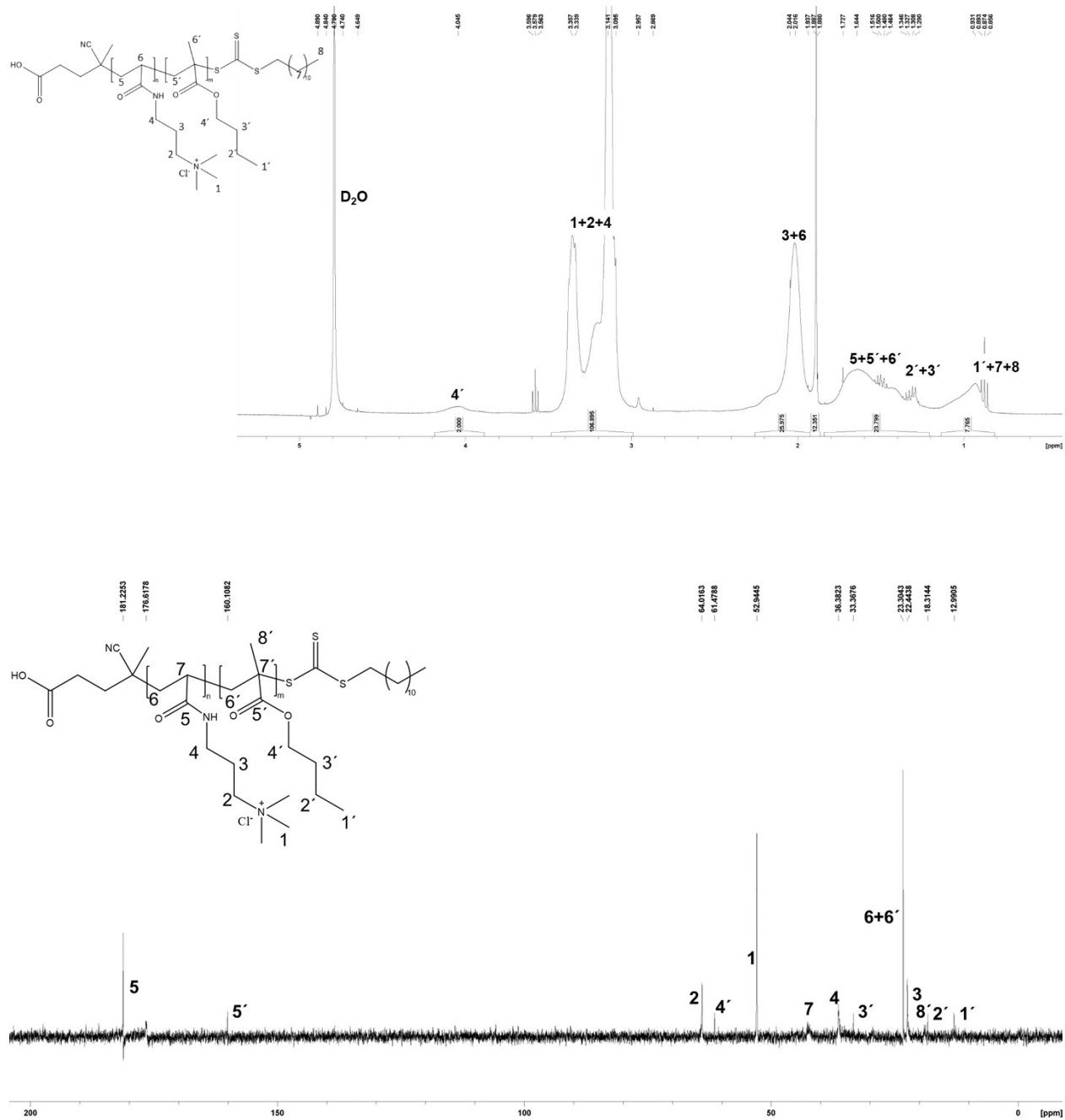


**Figure S5:** <sup>1</sup>H-NMR and <sup>13</sup>C-NMR of copolymer PAMPTMA-*r*-BuMA with 30 mol% of BuMA.



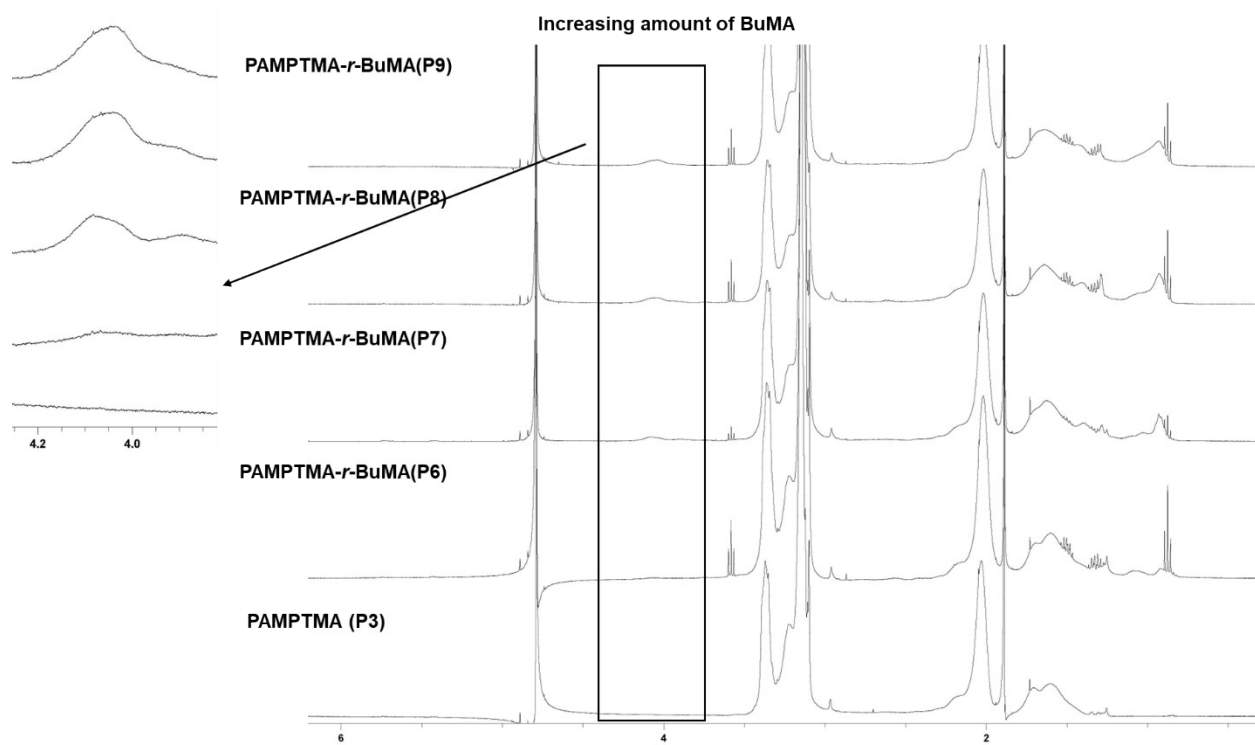


**Figure S6:** Confirmation of the increase in the hydrophobicity with the addition of the BuMA.

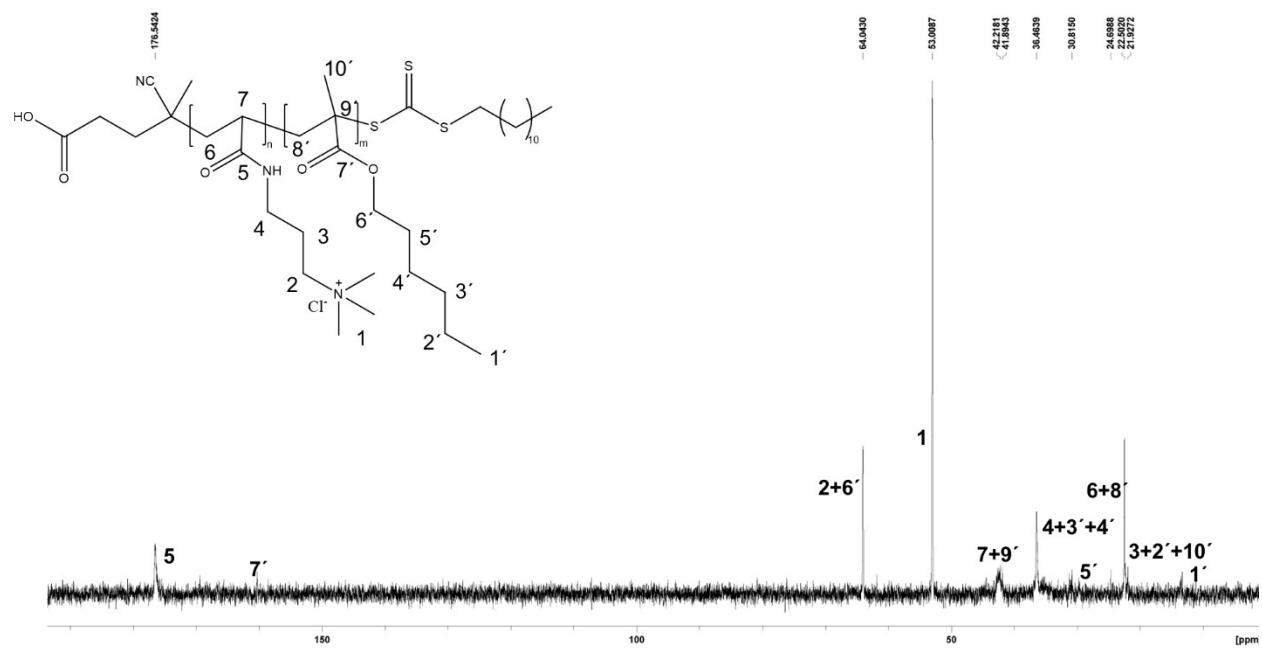
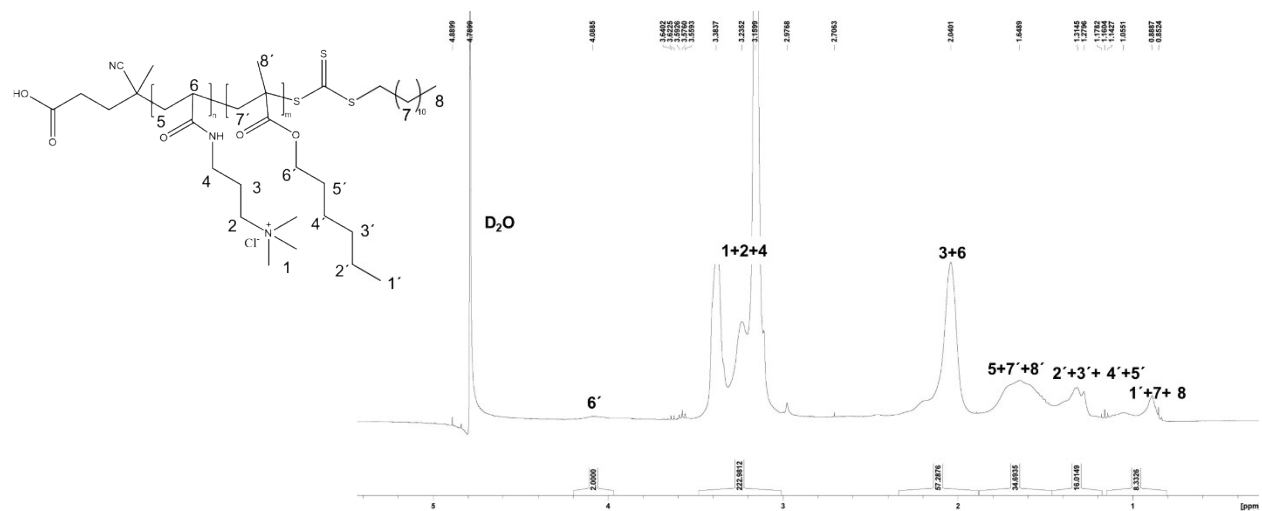


**Figure S7:** <sup>1</sup>H-NMR and <sup>13</sup>C-NMR of the copolymer of PAMPTMA-*r*-HexMA.

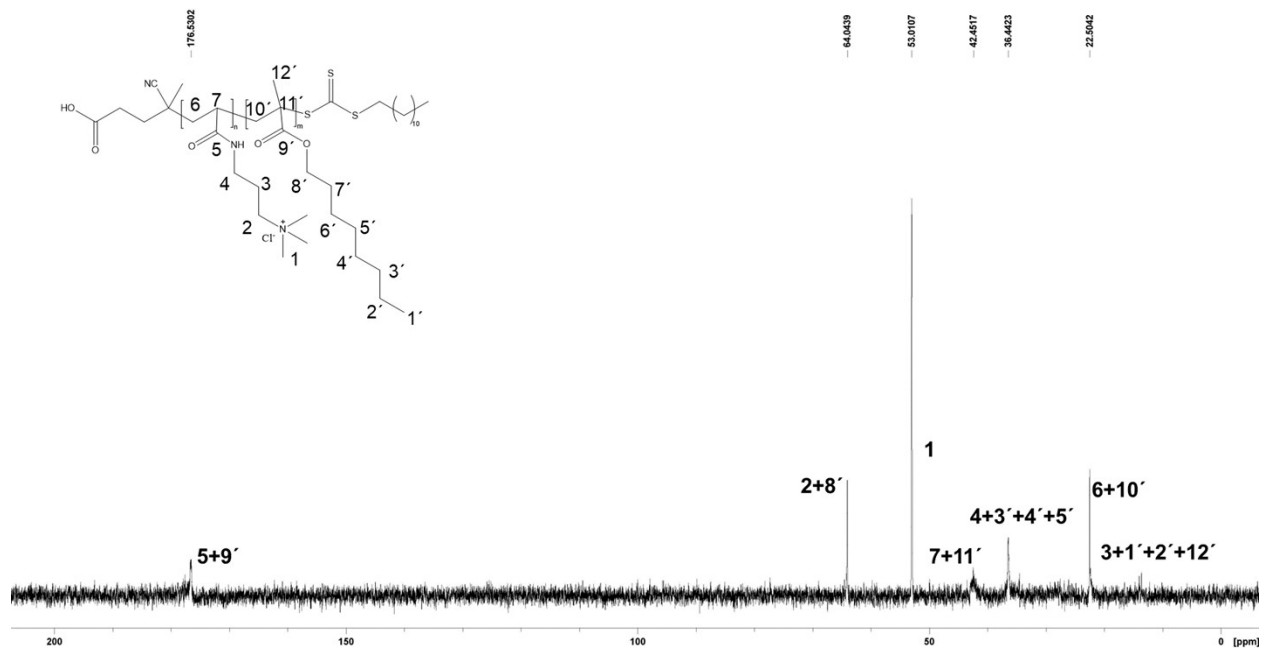
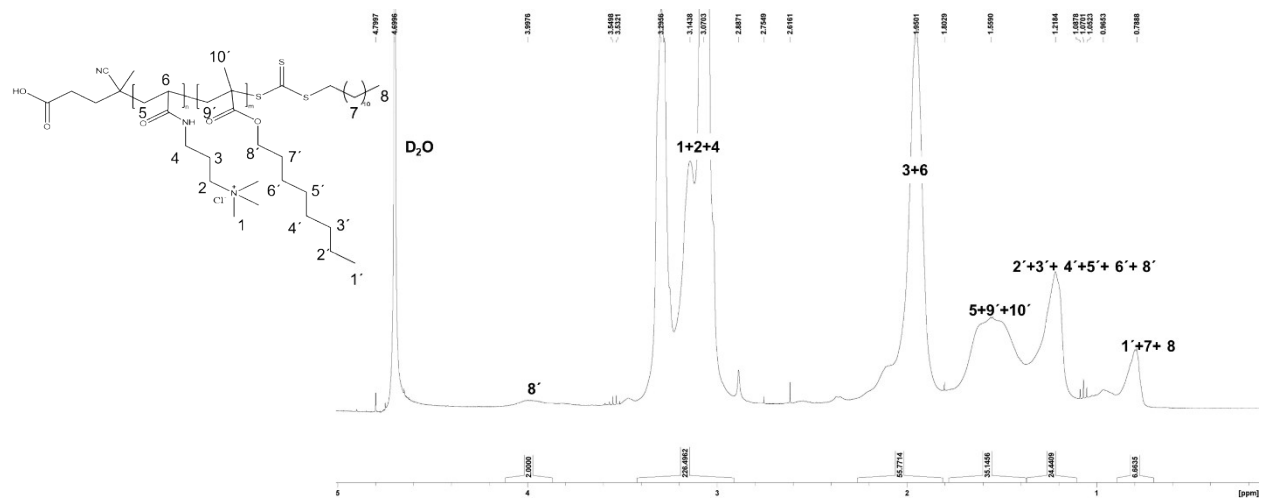
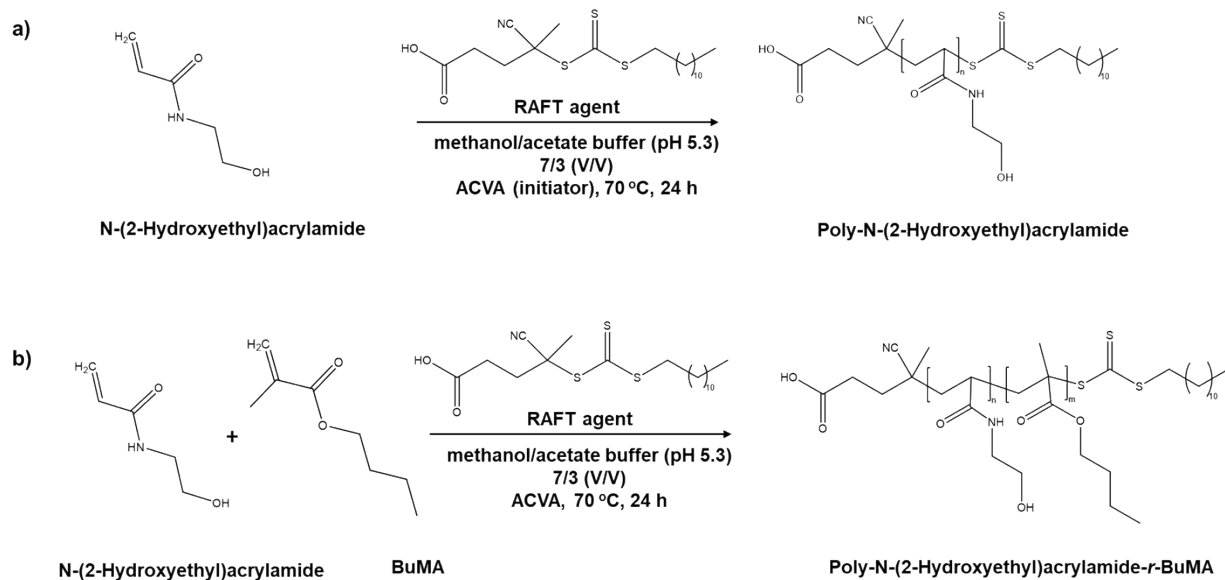


**Figure S8:** <sup>1</sup>H-NMR and <sup>13</sup>C-NMR of the copolymer of PAMPTMA-*r*-OctMA.



**Scheme S1:** Reaction scheme for the synthesis (a) homopolymers of N-(2-Hydroxyethyl)acrylamide (HEAA), and (b) copolymers of N-(2-Hydroxyethyl)acrylamide-*r*-BuMA.

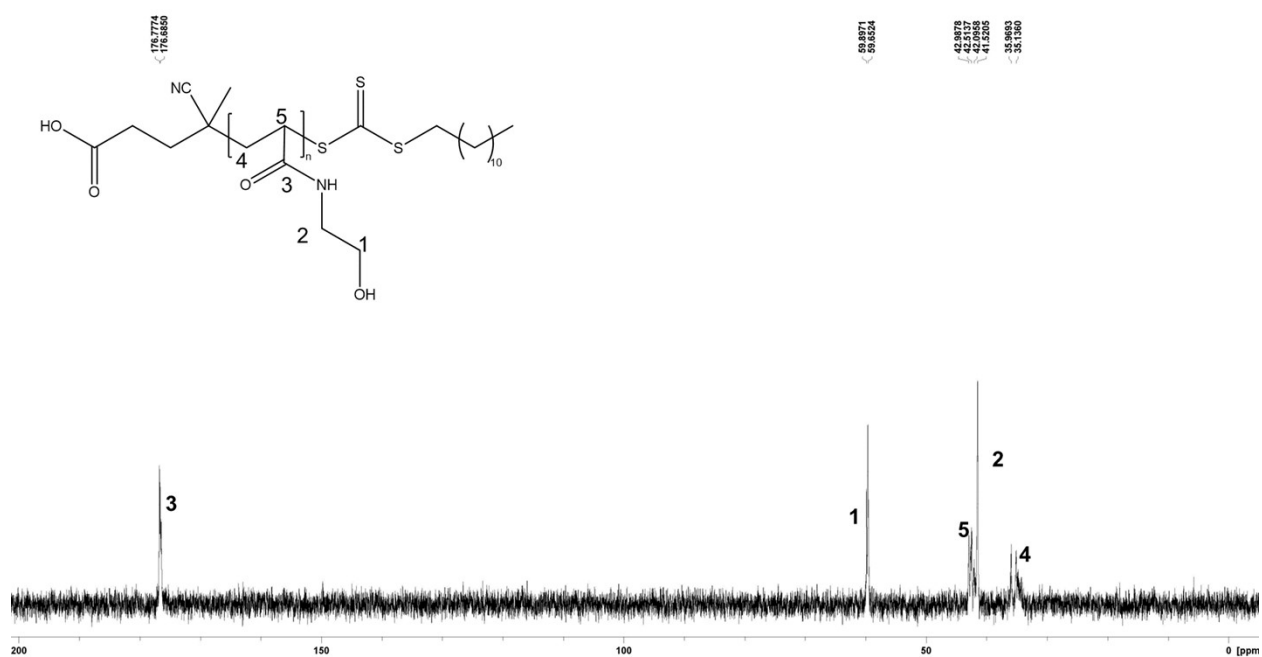
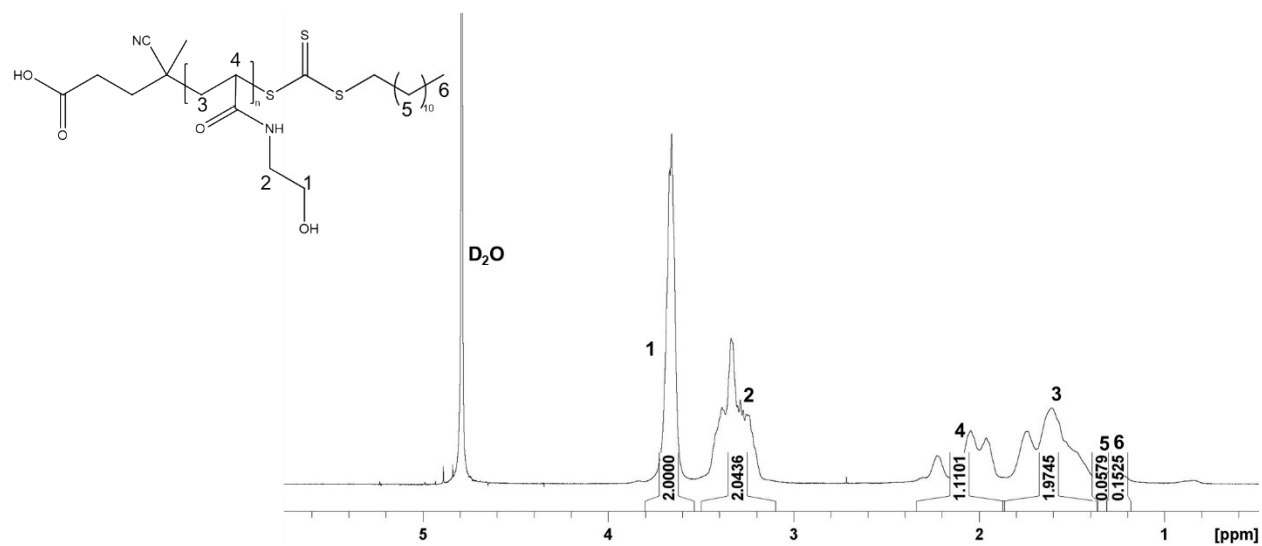


**Figure S9:** <sup>1</sup>H-NMR and <sup>13</sup>C-NMR of homopolymer of HEAA.

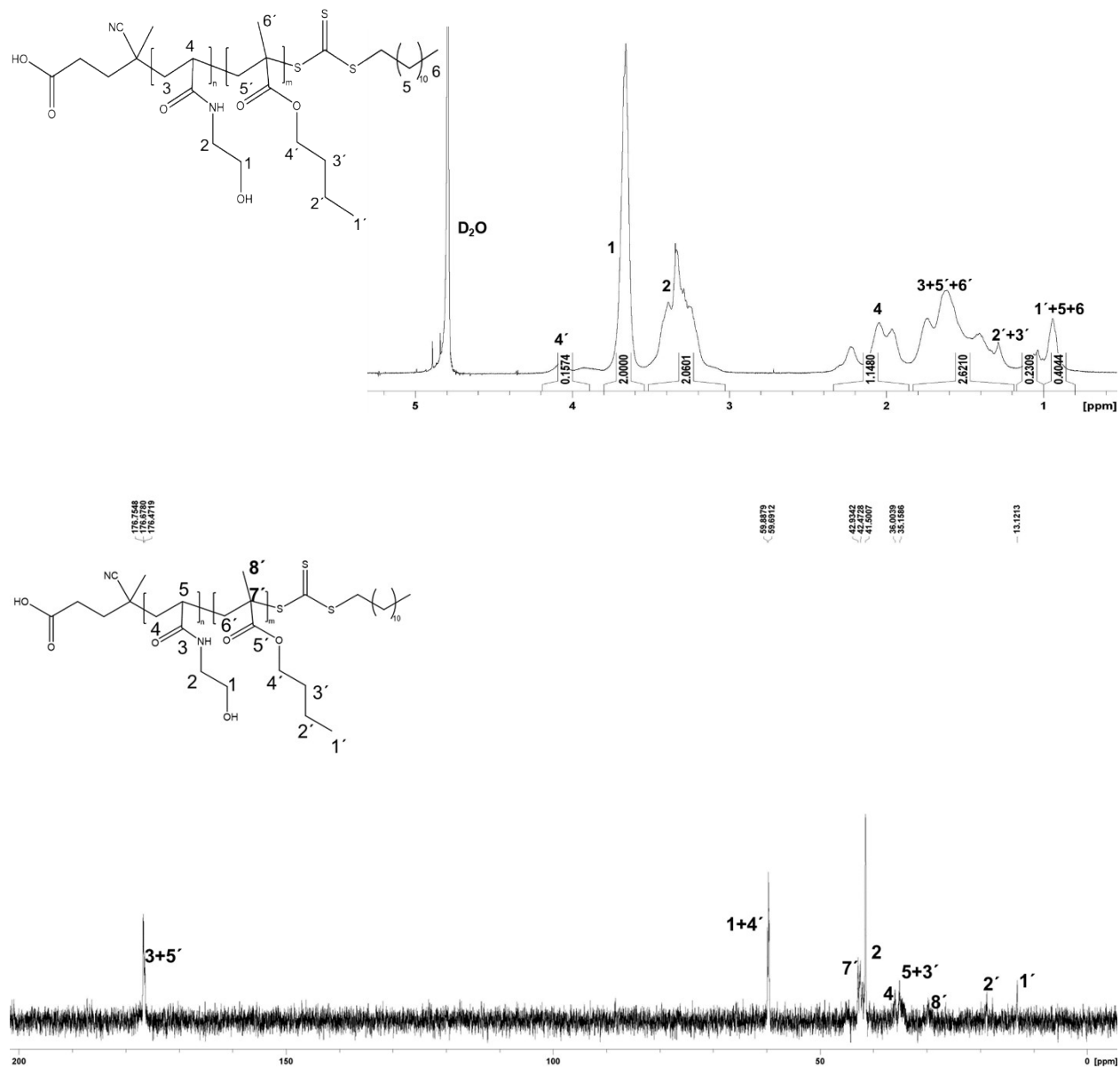


**Figure S10:** <sup>1</sup>H-NMR and <sup>13</sup>C-NMR of copolymer of HEAA with 10 mol% BuMA.

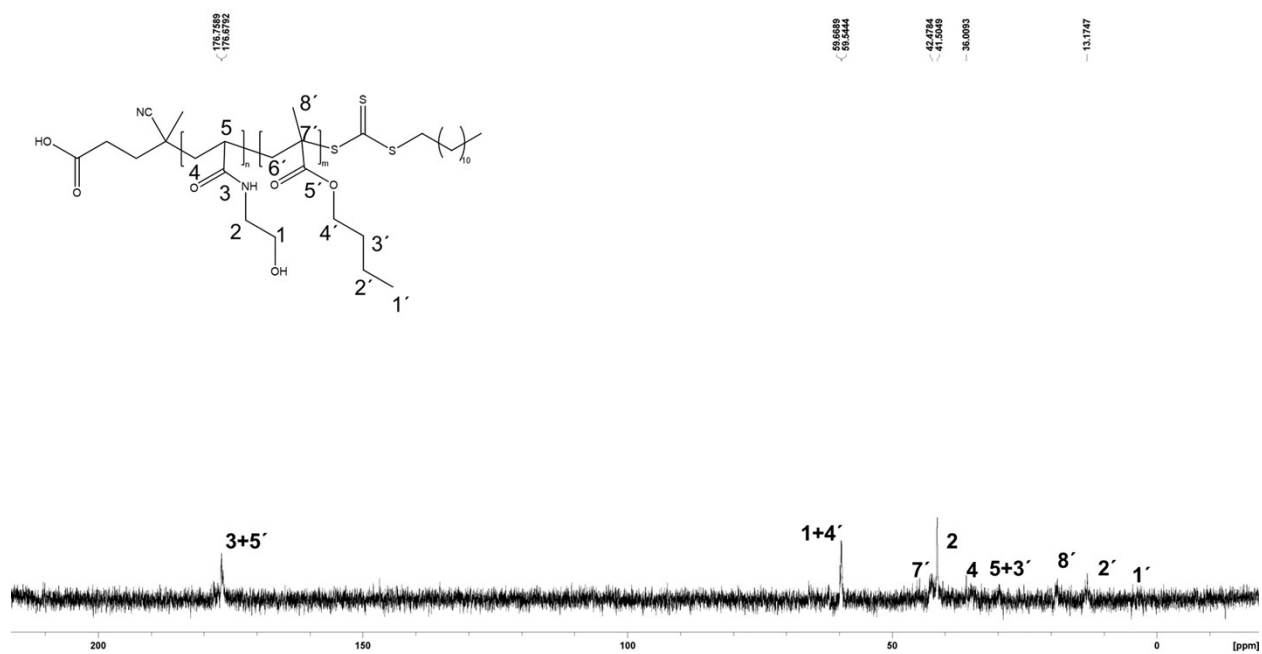
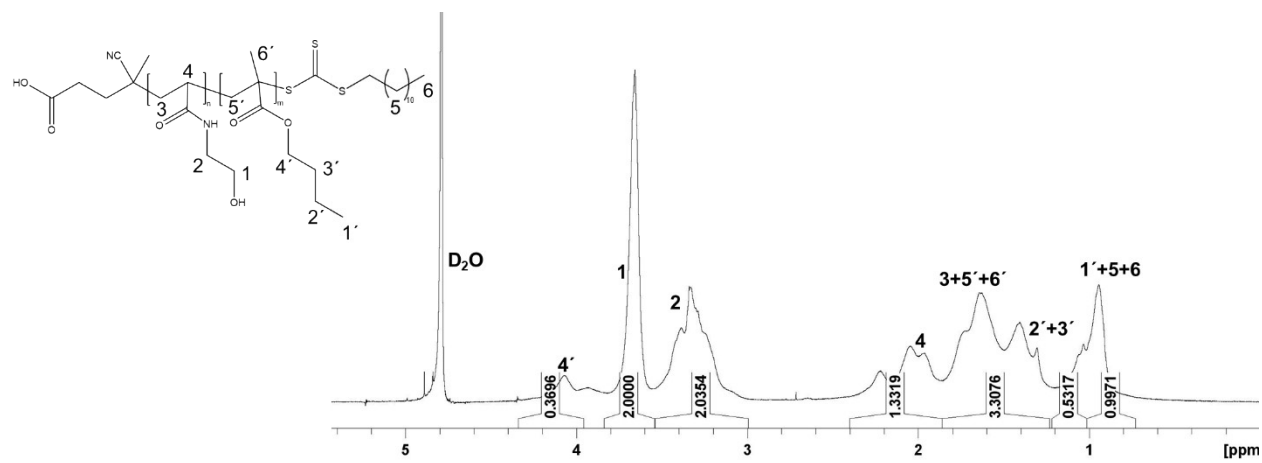


**Figure S11:**  $^1\text{H-NMR}$  and  $^{13}\text{C-NMR}$  of copolymer of HEAA with 20 mol% BuMA.

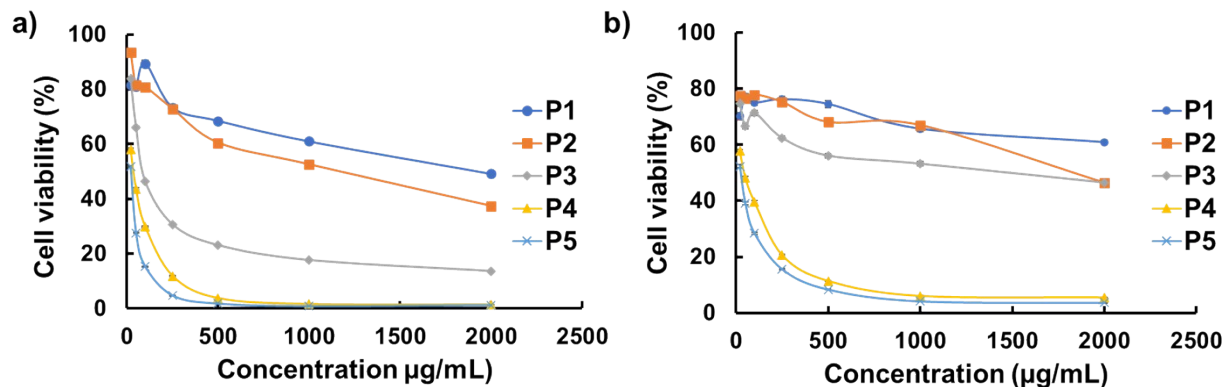


**Figure S12:** MTT cell viability assay of homopolymers PAMPTMA a.) Colon 26 cancer cell line, b.) and B16F10 cancer cell line.

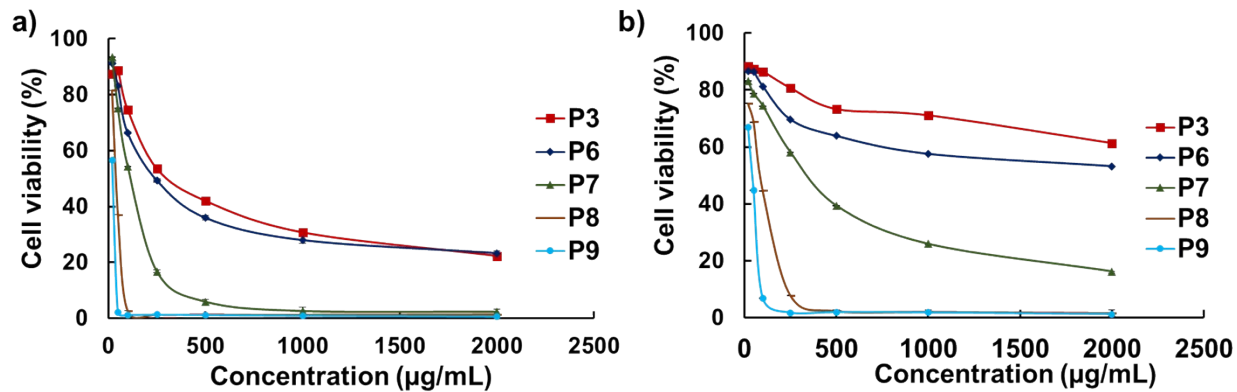


**Figure S13:** MTT cell viability assay of copolymers PAMPTMA-*r*-BuMA, a.) on Colon 26 cancer cell line, b.) on B16F10 cancer cell line.

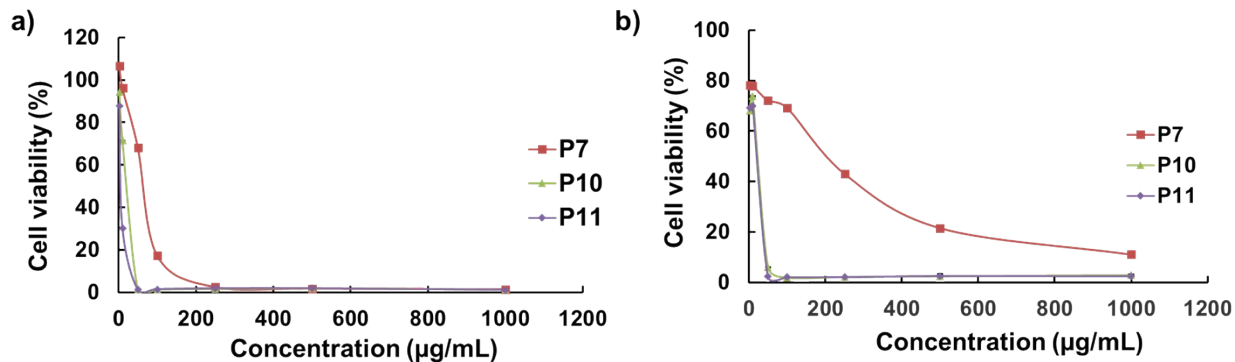


**Figure S14:** MTT cell viability assay of copolymers PAMPTMA-*r*-BuMA, PAMPTMA-*r*-HexMA, PAMPTMA-*r*-OctMA, a.) on Colon 26 cancer cell line, b.) on B16F10 cancer cell line.



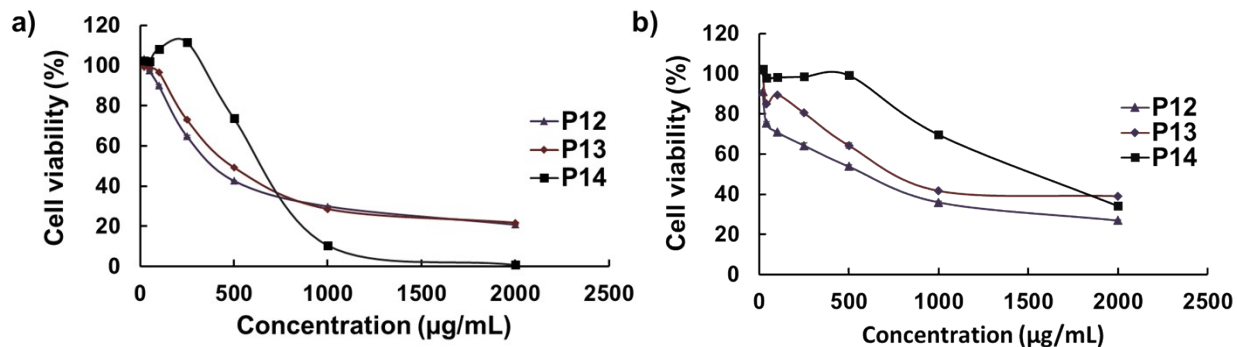


**Figure S15:** MTT cell viability assay of homo- and copolymers of HEAA, a.) on Colon 26 cancer cell line and b.) on B16F10 cancer cell line.

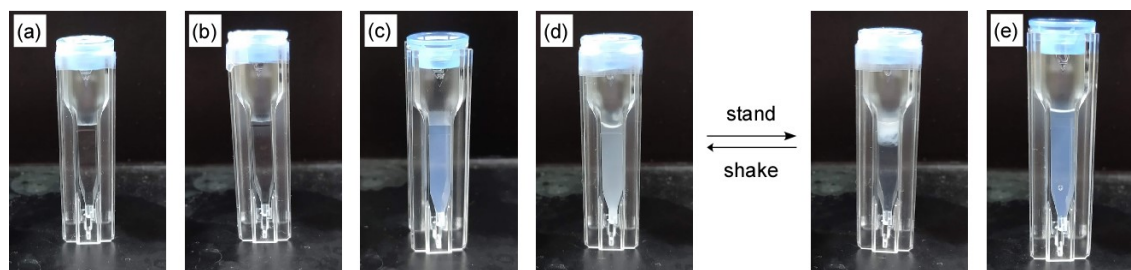


**Figure S16:** Photographs of (a) PAMPTMA (P3), (b) PAMPTMA-*r*-BuMA (P8), (c) DOPC, (d) mixture of DOPC/PAMPTMA, and (e) DOPC/PAMPTMA-*r*-BuMA in D<sub>2</sub>O. Concentrations were fixed at 1 g/L.

## References

1. D. S. BIOVIA, <https://www.3ds.com/products-services/biovia/products/molecular-modeling-simulation/biovia-materials-studio>.
2. J. Wang, P. Cieplak and P. A. Kollman, *Journal of Computational Chemistry*, 2000, **21**, 1049-1074.
3. A. D. Becke, *The Journal of Chemical Physics*, 1993, **98**, 5648-5652.
4. C. Lee, W. Yang and R. G. Parr, *Physical Review B*, 1988, **37**, 785-789.
5. R. Ditchfield, W. J. Hehre and J. A. Pople, *The Journal of Chemical Physics*, 1971, **54**, 724-728.
6. M. J. Frisch, G. W. Trucks, H. B. Schlegel, G. E. Scuseria, M. A. Robb, J. R. Cheeseman, G. Scalmani, V. Barone, G. A. Petersson, H. Nakatsuji, X. Li, M. Caricato, A. V. Marenich, J. Bloino, B. G. Janesko, R. Gomperts, B. Mennucci, H. P. Hratchian, J. V. Ortiz, A. F. Izmaylov, J. L. Sonnenberg,

- Williams, F. Ding, F. Lipparini, F. Egidi, J. Goings, B. Peng, A. Petrone, T. Henderson, D. Ranasinghe, V. G. Zakrzewski, J. Gao, N. Rega, G. Zheng, W. Liang, M. Hada, M. Ehara, K. Toyota, R. Fukuda, J. Hasegawa, M. Ishida, T. Nakajima, Y. Honda, O. Kitao, H. Nakai, T. Vreven, K. Throssell, J. A. Montgomery Jr., J. E. Peralta, F. Ogliaro, M. J. Bearpark, J. J. Heyd, E. N. Brothers, K. N. Kudin, V. N. Staroverov, T. A. Keith, R. Kobayashi, J. Normand, K. Raghavachari, A. P. Rendell, J. C. Burant, S. S. Iyengar, J. Tomasi, M. Cossi, J. M. Millam, M. Klene, C. Adamo, R. Cammi, J. W. Ochterski, R. L. Martin, K. Morokuma, O. Farkas, J. B. Foresman and D. J. Fox, *Journal*, 2016.
7. S. Jo, T. Kim, V. G. Iyer and W. Im, *Journal of Computational Chemistry*, 2008, **29**, 1859-1865.
  8. J. Wang, W. Wang, P. A. Kollman and D. A. Case, *Journal of Molecular Graphics and Modelling*, 2006, **25**, 247-260.
  9. H. M. A. D.A. Case, K. Belfon, I.Y. Ben-Shalom, J.T. Berryman, S.R. Brozell, D.S. Cerutti, T.E. Cheatham, III, G.A. Cisneros, V.W.D. Cruzeiro, T.A. Darden, R.E. Duke, G. Giambasu, M.K. Gilson, H. Gohlke, A.W. Goetz, R. Harris, S. Izadi, S.A. Izmailov, K. Kasavajhala, M.C. Kaymak, E. King, A. Kovalenko, T. Kurtzman, T.S. Lee, S. LeGrand, P. Li, C. Lin, J. Liu, T. Luchko, R. Luo, M. Machado, V. Man, M. Manathunga, K.M. Merz, Y. Miao, O. Mikhailovskii, G. Monard, H. Nguyen, K.A. O'Hearn, A. Onufriev, F. Pan, S. Pantano, R. Qi, A. Rahnamoun, D.R. Roe, A. Roitberg, C. Sagui, S. Schott-Verdugo, A. Shajan, J. Shen, C.L. Simmerling, N.R. Skrynnikov, J. Smith, J. Swails, R.C. Walker, J. Wang, J. Wang, H. Wei, R.M. Wolf, X. Wu, Y. Xiong, Y. Xue, D.M. York, S. Zhao, and P.A. Kollman *Journal*, 2022.
  10. E. L. Wu, X. Cheng, S. Jo, H. Rui, K. C. Song, E. M. Dávila-Contreras, Y. Qi, J. Lee, V. Monje-Galvan, R. M. Venable, J. B. Klauda and W. Im, *Journal of Computational Chemistry*, 2014, **35**, 1997-2004.
  11. S. Jo, J. B. Lim Jb Fau - Klauda, W. Klauda Jb Fau - Im and W. Im. *Biophysical Journal*, 2009, **97**, 50-58
  12. S. Jo, W. Kim T Fau - Im and W. Im. *PLoS ONE*, 2007, **9**, e880.
  13. J. Lee, D. S. Patel, J. Ståhle, S.-J. Park, N. R. Kern, S. Kim, J. Lee, X. Cheng, M. A. Valvano, O. Holst, Y. A. Knirel, Y. Qi, S. Jo, J. B. Klauda, G. Widmalm and W. Im, *Journal of Chemical Theory and Computation*, 2019, **15**, 775-786.
  14. B. R. Brooks, C. L. Brooks Iii, A. D. Mackerell Jr, L. Nilsson, R. J. Petrella, B. Roux, Y. Won, G. Archontis, C. Bartels, S. Boresch, A. Caflisch, L. Caves, Q. Cui, A. R. Dinner, M. Feig, S. Fischer, J. Gao, M. Hodoscek, W. Im, K. Kuczera, T. Lazaridis, J. Ma, V. Ovchinnikov, E. Paci, R. W. Pastor, C.

- B. Post, J. Z. Pu, M. Schaefer, B. Tidor, R. M. Venable, H. L. Woodcock, X. Wu, W. Yang, D. M. York and M. Karplus, *Journal of Computational Chemistry*, 2009, **30**, 1545-1614.
15. J. Lee, X. Cheng, J. M. Swails, M. S. Yeom, P. K. Eastman, J. A. Lemkul, S. Wei, J. Buckner, J. C. Jeong, Y. Qi, S. Jo, V. S. Pande, D. A. Case, C. L. Brooks, III, A. D. MacKerell, Jr., J. B. Klauda and W. Im, *Journal of Chemical Theory and Computation*, 2016, **12**, 405-413.